Comparison of high-order-harmonic generation on single-layer graphene flakes with armchair and zigzag types in an intense laser field

Jing Guo,[1,2,*] Huiying Zhong,[1,2] Bing Yan,[1,2] Yi Chen,[1,2] Yuanfei Jiang,[1,2] Ting-feng Wang,[3] Jun-feng Shao,[3] Chang-bin Zheng,[3] and Xue-Shen Liu[1,2,†]

[1]*Institute of Atomic and Molecular Physics, Jilin University, Changchun 130012, People's Republic of China*

[2]*Jilin Provincial Key Laboratory of Applied Atomic and Molecular Spectroscopy, Jilin University, Changchun 130012, People's Republic of China*

[3]*State Key Laboratory of Laser Interaction with Matter, Changchun Institute of Optics, Fine Mechanics and Physics, Chinese Academy of Sciences, People's Republic of China 130033*

(Received 22 April 2015; published 2 March 2016)

The high-order-harmonic generation (HHG) of graphene in an intense laser field is investigated using the strong-field approximation method. The initial wave function is presented by GAUSSIAN and GAMESS software. The molecular structure along the x and y axes represents different types of graphene: armchair and zigzag, respectively. The results show that the HHG intensity of the armchair type of graphene is two magnitudes higher than that of the zigzag type in the plateau area. The ionization yield and electron density distribution are also presented to further explain this difference. Finally, by superposing a properly selected range of harmonics, a main pulse with the duration of 91 and 99 attoseconds accompanied by weak satellite pulses will be generated for the case of armchair and zigzag graphene, respectively, and the corresponding intensity from armchair graphene is much higher than that from zigzag graphene.

DOI: 10.1103/PhysRevA.93.033806

I. INTRODUCTION

The nature of photoelectron dynamics has both practical and fundamental interest [1–3]. High-order-harmonic generation (HHG), which occurs during the process of laser pulses interacting with atoms or molecules, has been intensively studied for more than two decades because of its potential applications for generating coherent extreme ultraviolet (XUV) light sources [4–6]. The HHG photons define a subfemtosecond coherent electromagnetic field which is completely in phase with the driving laser pulse. Thus, experiments taking advantage of selective HHG have produced a new coherent light source which can probe electronic processes on the attosecond time scale. The HHG process can be semiclassically described by a three-step model where the electron first undergoes tunnel ionization, after which it propagates in the field gaining energy, and finally returns to the parent ion and recombines, emitting a high-energy photon [7]. In quantum mechanics this process can be analyzed by the strong-field approximation (SFA) theory [8,9]. The photon intensity spectrum from the SFA method gives a plateau structure of HHG photons up to a maximum cutoff frequency.

In recent years, the successful preparation of single-layer graphene [10] has led to a worldwide investigation of carbonaceous material [11–16]. Graphene has recently become a unique material for studying light-matter interaction effects in low-dimensional electric systems. Owing to a gapless linear band structure and a high mobility of massless charge carriers, graphene is widely recognized as a future material for all-wavelength optoelectronics. Being of strong fundamental importance, these effects also open a wide range of opportunities in photonics and optoelectronics [10,17,18]. Besides, graphene has received intense attention in both fundamental and applied sciences [19], and is considered to be a promising material for nonlinear optics in nanostructures [20,21]. For example, it has been demonstrated that HHG spectra from a simple graphene model represent strong signals at maximum cutoff order for linearly as well as coplanar-circularly polarized pulses of a driving laser field [22,23].

In this paper, we present calculations of HHG spectra from graphene interacting with linearly polarized laser pulses by the molecular Lewenstein method. We will investigate HHG from graphene molecules of armchair and zigzag types in intense laser fields. We will also investigate ionization yield and electron density distribution to interpret this phenomenon and explain this difference of dynamics between armchair and zigzag graphene molecules. In addition, by the superposition of HHG near the cutoff region, an isolated 91-attosecond pulse can be generated.

II. THEORETICAL METHOD

Single-layer graphene is an extended two-dimensional structure defined by carbon atoms in a hexagonal honeycomb lattice with sp^2 hybridization. The thickness is only 0.335 nm, and the C-C bond length is 0.142 nm, which is the thinnest material in the world at present. The carbon atoms in graphene are connected by a strong σ bond, giving graphene excellent tensile strength; the C-C bond is not likely to be broken in the external tensile force, thus the graphene lattice can remain relatively stable. On the other hand, the bending stiffness of graphene is relatively low [16], so it can bend under small external force. The mechanical properties along the x and y axes of single-layer graphene are quite different, which are defined as armchair and zigzag types of graphene, respectively. Figure 1 presents the molecular structure of single-layer graphene, which can be obtained by GAUSSIAN and GAMESS

*gjing@jlu.edu.cn
†liuxs@jlu.edu.cn

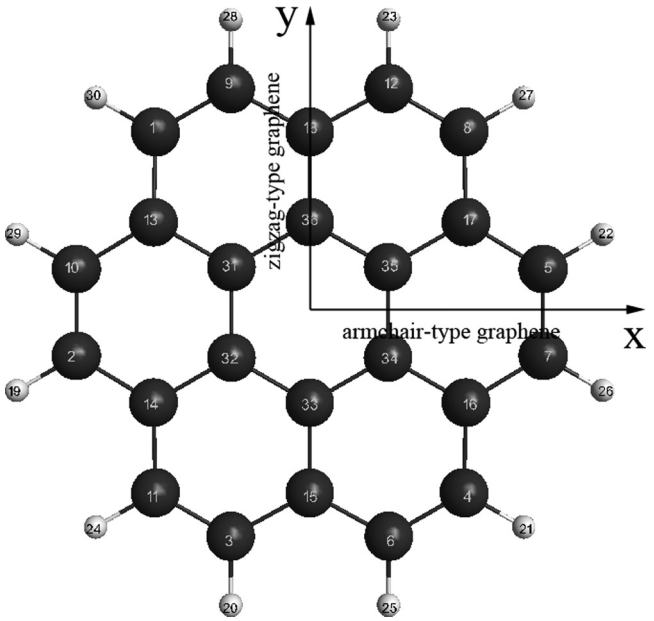

FIG. 1. Molecular structure of a single-layer graphene flake.

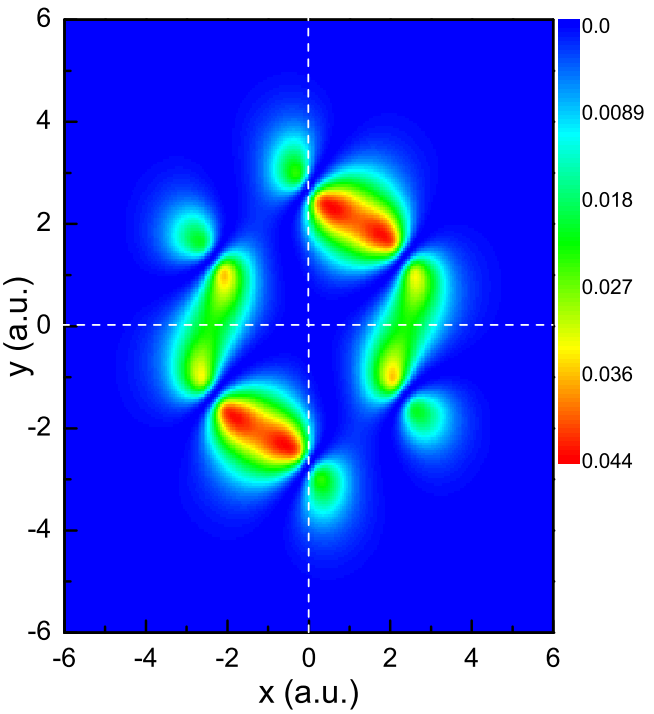

FIG. 2. Electron density of the HOMO of a single-layer graphene flake, where the two white dashed lines represent the x and y axes.

software [24]. We can see from Fig. 1 that in our model of a graphene layer, 36 atoms are chosen, which consists of 24 C atoms (big black ball in Fig. 1) and 12 H atoms (small white ball in Fig. 1), and we focus on the six C atoms in the center ring, which have the representative character of graphene.

The strong-field approximation is based on three assumptions: The dominant contribution to HHG comes from electrons that (1) return to the nucleus, (2) appear in the continuum with zero velocity, and (3) have an appropriate kinetic energy to produce a given harmonic at the time of return. This classical interpretation shows that in order to control high-order-harmonic generation processes, one should try to control the motion of free electrons in the laser field. The strong-field Lewenstein model for molecules has been widely used before and has been applied to small molecules such as N_2, O_2, and CO_2 [25–28]. Recently, it also has been applied to larger systems such as the chiral molecules camphor and fenchone [29]. We choose the single-layer graphene flake and just consider its highest occupied molecular orbital (HOMO), and base our approach on the explicit expression in Ref. [30]. The initial state of the active electron is the HOMO, the ionization energy of which is -0.4556 a.u., i.e., $|\Psi_0\rangle$. Figure 2 shows the HOMO of graphene, which is the sum of two degenerated states which have the same energy -0.4556 a.u., and this corresponds to the HOMO of graphene. We can see from Fig. 2 that the density distribution is symmetric and the strength along the x axis is much larger than that along the y axis. The overall transition amplitude will be the sum

$$M = \sum_{j,j} M_{jj} + \text{c.c.}, \tag{1}$$

and explicitly,

$$M_{jj} = -iC_j^* C_j \int_{-\infty}^{\infty} dt \int_{-\infty}^{t} dt' \int d^3p\, d_z^{*(j)}(\mathbf{p}+\mathbf{A}(t)) \times d_z^{(j)}(\mathbf{p}+\mathbf{A}(t'))\exp\left(iS(t,t',\mathbf{p})\right). \tag{2}$$

where $d_z^{(j)}(\mathbf{p}) = \langle \mathbf{p}|\mathbf{r}\cdot\hat{e}_z|j\rangle$ are the components of the dipole matrix elements related to the orbitals $|j\rangle$ along the field-polarization axis.

In the above equations, the amplitudes M_{jj} correspond to the processes in which the electron leaves one orbital and reaches a Volkov state, then comes back and recombines with the same orbital. The corresponding classical action reads

$$S(t,t',\mathbf{p}) = \Omega t - \frac{1}{2}\int_{t'}^{t} d\tau[\mathbf{p}+\mathbf{A}(\tau)]^2 - E_\alpha(t-t'), \tag{3}$$

where E_α represents the bound-state energies, t and t' the recombination and start times, respectively, and $\mathbf{p}$ the intermediate momentum. Ω is the high-harmonic radiation frequency. In Eq. (3), recombination time determines the instant when the electron combines with the parent ion. The above equation describes a physical process in which an electron, initially in a field-free bound state, is coupled to a Volkov state by the interaction between the system and the field. Subsequently, it propagates in the continuum and is driven back toward its parent ion, with which it recombines at a time t, emitting high harmonics.

III. RESULTS AND DISCUSSION

In our simulation, the expression for the linearly polarized laser field is

$$E(t) = E_0 f(t)\cos(\omega t+\phi), \tag{4}$$

where $f(t) = \exp[-2\ln 2(t-T/2)^2/\tau_d^2]$ is the pulse envelope, E_0 and ω are the amplitude and frequency of the laser field, and $\phi = 0$ is the relative phase. The length of time t for the time evolution is $T = 12T_0$ and $\tau_d = 5$ fs, where T_0

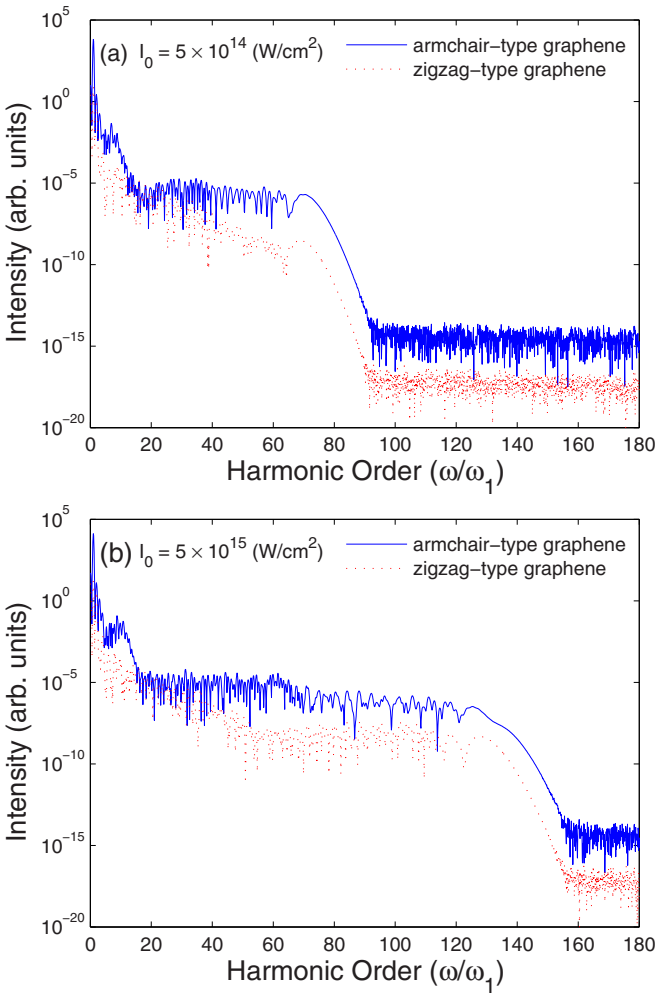

FIG. 3. Harmonic spectra from armchair and zigzag graphene molecules in intense laser fields, where (a) and (b) present laser intensity $I_0 = 5 \times 10^{14}$ W/cm^2 and $I_0 = 1 \times 10^{15}$ W/cm^2 cases, respectively.

is the optical cycle of a 800-nm pulse. The laser direction along the x or y axis represents armchair or zigzag graphene, respectively [11].

Figure 3 shows HHG from armchair and zigzag graphene molecules in intense laser fields, respectively. We can see from Fig. 3 that for both cases the HHG spectra present a plateau structure until the cutoff region. The HHG cutoffs for both cases are almost the same, which is about 80 harmonic order at intensity $I_0 = 5 \times 10^{14}$ W/cm^2 and about 130 at intensity $I_0 = 1 \times 10^{15}$ W/cm^2. Furthermore, there are some distinct differences in the HHG spectra. We can see from Figs. 3(a) and 3(b) that compared with the zigzag graphene case, the HHG intensity is enhanced with the armchair graphene molecule, especially for the high-energy region of HHG. This is because the initial electron density along the x axis (corresponding to armchair graphene) is much larger than that along the y axis (zigzag graphene) (see Fig. 2), which causes the big difference between the HHG for the armchair and zigzag graphenes.

To further understand the different physical mechanisms of HHG in the armchair and zigzag graphene cases, we also

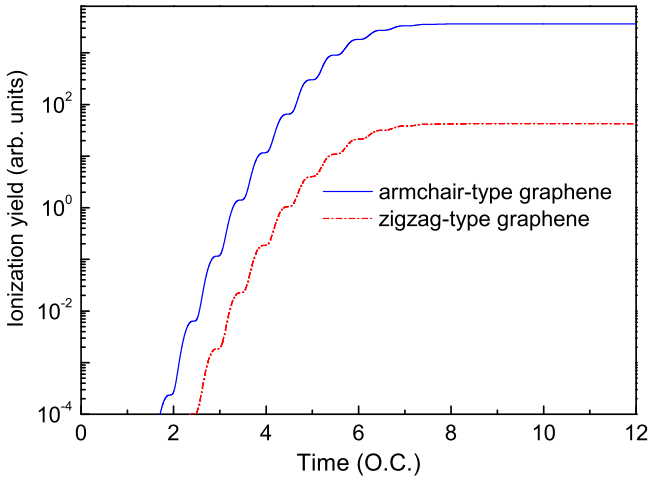

FIG. 4. Ionization yield as a function of time (in optical cycles) with armchair and zigzag graphenes at $I_0 = 1 \times 10^{15}$ W/cm^2.

give a clear physical picture in terms of ionization yield as the function of time with armchair and zigzag graphene at $I_0 = 1 \times 10^{15}$ W/cm^2 (see Fig. 4). The results also show that the ionization yield of armchair graphene is much larger than that of zigzag graphene, which is also in accordance with the HHG and electron density distribution.

The attosecond pulse is produced by simply making an inverse Fourier transformation without any phase compensation. Figure 5 shows attosecond generation with armchair and zigzag graphenes. By superposing a properly selected range of harmonics, a main pulse with the duration of 91 and 99 as accompanied by weak satellite pulses will be generated for the case of armchair and zigzag graphene molecules, respectively. From Fig. 5 we can see for armchair graphene a main attosecond pulse is generated, but it is accompanied by some weak satellite pulses, and the generation time is in accordance with time-frequency analysis. Two peaks are generated by the short and long quantum paths. For zigzag

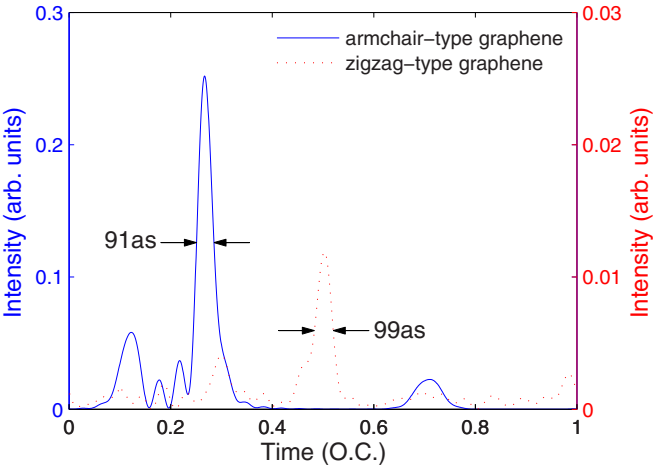

FIG. 5. Temporal profiles of the attosecond pulses generated by superposing harmonics from 103th to 132th order harmonics for armchair graphene and from 42th to 68th order harmonics for zigzag graphene.

graphene there are two main attosecond pulses generated, and the generation times of the two peaks are 0.3 and 0.5 optical cycles (o.c.). Besides, the intensity from the armchair graphene molecule is much larger than that from the zigzag molecule, which is also in accordance with HHG.

IV. CONCLUSIONS

In summary, we investigated the high-order-harmonic generation and isolated attosecond pulse from armchair and zigzag graphene molecules. The initial state is well described by the GAUSSIAN wave packet which can present an explicit structure of a single-layer graphene molecule. We calculated the HHG of HOMOs of graphene and the results show that the HHG can be enhanced with armchair graphene, which can be well explained by the fact that initial electron density distribution along the x axis is much larger than that along the y axis. The ionization yield of armchair graphene is much larger than that of zigzag graphene, which also confirmed the above point. In addition, we also investigated the attosecond pulse generation on HHG. With such a spectrum, attosecond pulses with durations of 91 and 99 as would be achieved straightforwardly with zigzag and armchair graphenes, respectively.

ACKNOWLEDGMENTS

This work was supported by National Natural Science Foundation of China under Grants No. 11574117, No. 11271158, No. 61575077, and No. 11204103, and also partially supported by the Research Foundation of National Defense (No. 419140100023, 419140100048), and the Excellent Young Scientist Foundation (No. 450060521231).

[1] M. Uiberacker *et al.*, Nature (London) **446**, 627 (2007).
[2] J. Heslar, D. Telnov, and S.-I. Chu, Phys. Rev. A **83**, 043414 (2011).
[3] P. B. Corkum and F. Krausz, Nat. Phys. **3**, 381 (2007).
[4] R. A. Bartels, A. Paul, H. Green *et al.*, Science **297**, 376 (2002).
[5] T. Popmintchev *et al.*, Science **336**, 1287 (2012).
[6] Y. Pan, S.-F. Zhao, and X.-X. Zhou, Phys. Rev. A **87**, 035805 (2013).
[7] P. B. Corkum, Phys. Rev. Lett. **71**, 1994 (1993).
[8] M. Lewenstein, P. Balcou, M. Y. Ivanov, A. L'Huillier, and P. B. Corkum, Phys. Rev. A **49**, 2117 (1994).
[9] P. B. Corkum, N. H. Burnett, and F. Brunel, Phys. Rev. Lett. **62**, 1259 (1989).
[10] K. S. Novoselov, A. K. Geim, S. V. Morozov *et al.*, Science **306**, 666 (2004).
[11] L. Y. Huang and Q. Han, Sin-Phys. Mech. Astron. **42**, 319 (2012).
[12] Y. W. Gao and P. Hao, Physica E **41**, 1561 (2009).
[13] M. Sadeghi and R. Naghdabadi, Nanotechnology **21**, 105705 (2010).
[14] Q. Wang and K. M. Liew, Phys. Lett. A **363**, 236 (2007).
[15] S. C. Pradhan, Phys. Lett. A **373**, 4182 (2009).
[16] Q. Z. Yuan and Y. P. Zhao, Phys. Rev. Lett. **104**, 246101 (2010).
[17] K. S. Novoselov *et al.*, Nature **490**, 192 (2012).
[18] F. Bonaccorso, Z. Sun, T. Hasan, and A. C. Ferrari, Nat. Photon. **4**, 611 (2010).
[19] A. K. Geim and K. S. Novoselov, Nat. Mater. **6**, 183 (2007).
[20] Y. Q. An, F. Nelson, J. U. Lee, and A. C. Diebold, Nano Lett. **13**, 2104 (2013).
[21] M. Sivis, M. Duwe, B. Abel, and C. Ropers, Nat. Phys. **9**, 304 (2013).
[22] S. A. Sørngård, S. I. Simonsen, and J. P. Hansen, Phys. Rev. A **87**, 053803 (2013).
[23] S. I. Simonsen, S. A. Sørngård, M. Førre, and J. P. Hansen, J. Phys. B **47**, 065401 (2014).
[24] GAMESS-UK is a package of *ab initio* programs. See http://www.cfs.dl.ac.uk/gamess-uk/index.shtml, and M. F. Guest, I. J. Bush, H. J. J. van Dam, P. Sherwood, J. M. H. Thomas, J. H. van Lenthe, R. W. A. Havenith, and J. Kendrick, Mol. Phys. **103**, 719 (2005).
[25] B. B. Augstein and C. Figueira de Morisson Faria, Mod. Phys. Lett. B **26**, 113002 (2012).
[26] Y. Yu, J. Xu, Y. Fu, H. Xiong, H. Xu, J. Yao, B. Zeng, W. Chu, J. Chen, Y. Cheng, and Z. Xu, Phys. Rev. A **80**, 053423 (2009).
[27] S.-F. Zhao, C. Jin, R. R. Lucchese, A.-T. Le, and C. D. Lin, Phys. Rev. A **83**, 033409 (2011).
[28] X. M. Tong, Z. X. Zhao, and C. D. Lin, Phys. Rev. A **66**, 033402 (2002).
[29] I. Dreissigacker and M. Lein, Phys. Rev. A **89**, 053406 (2014).
[30] J. Guo, X.-L. Ge, H. Zhong, X. Zhao, M. Zhang, Y. Jiang, and X.-S. Liu, Phys. Rev. A **90**, 053410 (2014).